Int. J. Heat Mass Transfer. Vol. 35, No. 11, pp. 3141–3151, 1992
Printed in Great Britain

0017–9310/92 $5.00 + 0.00
© 1992 Pergamon Press Ltd

Direct numerical solution of diffusion problems with intrinsic randomness

XIAOWEI S. HE and JOHN G. GEORGIADIS
Department of Mechanical Engineering and Materials Science, Duke University, Durham, NC 27706, U.S.A.

(*Received* 30 *November* 1990 *and in final form* 8 *August* 1991)

Abstract—A hybrid numerical–symbolic manipulation scheme is developed for the analysis of diffusion problems with intrinsic randomness. The scheme is applied in the study of one-dimensional heat conduction in fully-saturated packed beds in order to study the effects of packing disorder on the medium effective conductivity. Conduction is modeled by a parabolic partial differential equation with random local conductivity. Randomness originates from the spatial fluctuation of porosity near solid walls and in the bulk region. Assuming a certain porosity statistical distribution, the steady and unsteady heat conduction problems are solved. The steady-state solution is used to obtain both the mean value and the standard deviation of the effective conductivity for a range of fluid to solid conductivity ratios. The mean and standard deviation are used to interpret the scatter of experimental results found in the literature. The unsteady heat conduction equation is discretized on a finite spatial grid and an explicit integration in time is carried out symbolically for each time step.

INTRODUCTION

FROM THE point of view of continuum mechanics, statistical or non-deterministic methods offer the most economic framework for the analysis of systems with intrinsic randomness. Candidates for such systems are structures with complicated (or disordered) geometry, such as composite materials or porous media. Typical examples are fluid-saturated packed beds consisting of random packings of solid particles. We assume that transport processes in such media can be described by continuum models with spatially random parameters. Since the details of the microstructure are known only in an average (or statistical) sense, it is in the same sense that the solution of the governing equation is sought. For definiteness, consider diffusion of a passive scalar through a randomly packed bed. Given the exact location of the solid particles and the transport coefficients in the two phases (solid–fluid), one can (in principle) obtain the solution of the governing diffusion equation everywhere in the domain. Owing to the complexity of the microstructure and the uncertainty of packing (i.e. the method of assembling the packed bed), the exact solution is impossible to obtain in a deterministic sense. Furthermore, local information is redundant. All that is frequently required is an estimate of the average flux of the scalar and a description of its statistics. For example, the second moment (as expressed by the standard deviation) is required in addition to the mean value. The standard deviation gives a measure of the reliability of the mean value.

Uncertainties in materials properties and structural geometry can be mathematically modeled as stochastic processes in space, or random fields, cf. Vanmarcke [1]. Statistical descriptors for such fields in packed beds can be obtained, for example, from *in-situ* measurements, cf. Georgiadis [2], or analytical models of the packing, cf. Haughey and Beveridge [3]. Transport of a scalar in random fields can be described via partial differential equations with random parameters. Problems related to the formulation and analysis of stochastic transport equations were analyzed by researchers in the field of underground water transport, see review by Sposito *et al.* [4].

In general, solutions of stochastic differential equations are difficult to obtain because the solution is statistically correlated to the random parameters. In practice, solution methodologies for non-deterministic problems depend on the type of problem for which they were developed. We can conveniently divide available methodologies for problems with intrinsic randomness into two categories: (i) perturbation methods; and (ii) direct methods. The first category pertains to problems where the random part is weak, i.e. the random component is much smaller than the deterministic. Perturbation methods have been applied to structural analysis, cf. Benaroya and Rehak [5], and heat transfer, cf. Tzou [6, 7] and Georgiadis [8]. In general, 'weak randomness' models have a limited range of applicability. Let us consider, for example, the problem of heat conduction in a randomly packed bed consisting of a mixture of solid beads and a fluid. If the ratio of fluid to solid thermal conductivity λ is close to unity, a small perturbation scheme can be set up by using $(1-\lambda)$ as an infinitesimally small parameter. The convergence rate of the perturbation expansion can be improved only by including progressively more microstructural information on the packed bed, cf. Torquato [9]. It is

NOMENCLATURE

a	1.4, parameter of mean porosity profile, equation (7)
A, D	coefficients in equation (23), defined by equations (24) and (25)
b	2.0, parameter of mean porosity profile, equation (7)
B	porosity function, equation (5)
D_p	bead diameter [m]
$f(\tilde{\phi})$	probability density function of porosity
H	half width of the packed bed [m]
i, n	integers
K_0	reference effective conductivity, given by equation (4) with $\phi = \phi_0$ [W m^{-1} K^{-1}]
K_e	overall effective conductivity of packed bed [W m^{-1} K^{-1}]
K_e max	maximum estimate of overall conductivity, equation (30) [W m^{-1} K^{-1}]
K_e exp	experimental estimate of overall conductivity [W m^{-1} K^{-1}]
K_f	conductivity of the fluid phase [W m^{-1} K^{-1}]
K_s	conductivity of the solid phase [W m^{-1} K^{-1}]
K_x	local effective conductivity of packed bed [W m^{-1} K^{-1}]
K_x^*	K_x/K_0, non-dimensional local effective conductivity
N_t, N_x	total number of grid points in (t^*, X) space
q	heat flux [W m^{-2}]
t	time variable [s]
t^*	$tK_0/H^2(\rho c)_m$, non-dimensional time variable
T	temperature [K]
T_c, T_h	temperature at the left, right solid walls [K]
x	horizontal coordinate [m]
X	x/H, non-dimensional horizontal coordinate.

Greek symbols

α	32.30, probability density parameter, equation (8)
β	56.49, probability density parameter, equation (8)
γ	D_p/H, bead diameter-to-half width ratio
Δt	numerical time step
Δx	numerical mesh size
θ	$(T-T_c)/(T_h-T_c)$, non-dimensional temperature
λ	K_f/K_s, fluid-to-solid conductivity ratio
$(\rho c)_m$	heat capacity of the fluid-saturated packed bed [J m^{-3} K^{-1}]
ϕ	local porosity, equation (6)
ϕ_0	0.3, mean porosity in the core region
$\bar{\phi}$	deterministic component of local porosity
$\tilde{\phi}$	random component of local porosity, equation (6).

Special symbols

$\Gamma(\cdot)$	Gamma function
E[·], ⟨·⟩	mathematical expectation, mean value
SD[·]	standard deviation
REV	Representative Elementary Volume, Fig. 1(a).

obvious that such expansions do not converge for widely different conductivities. Moreover, it is very difficult to demonstrate convergence without using, for example, Monte Carlo simulations for comparison. Monte Carlo schemes form a whole class of direct methods for the solution of non-deterministic problems but such methods are notoriously inefficient for random fields; they will not concern us here.

The purpose of this article is to investigate a class of direct methods for the solution of diffusion problems characterized by stochastic differential equations and by finite random variation of transport coefficients. In general, numerical methods are required. Padovan and Guo [10] and Padovan *et al.* [11] introduced non-deterministic finite-difference and finite-element techniques in the solution of certain steady-state heat conduction and structural mechanics problems. They discretized the governing equations on a finite mesh, derived a linear algebraic system (via standard finite-element or -difference approximations), and then formally inverted the statistical matrix to obtain an explicit form of the solution. We feel that the method of Padovan and co-workers [10, 11] is a step in the right direction. However, it only treats 'sparsely probabilistic systems'; the formulation of the statistical terms is such that, after the discretization, the statistical matrix is not only sparse but it can also be decoupled into a sum of deterministic matrices, each multiplied by the random variable.

In this article, we propose a more general direct numerical method for the solution of non-deterministic diffusion problems. Although this method can be applied to a broad class of problems described by partial differential equations with random coefficients, we choose to apply it to the heat conduction problem in fluid-saturated packed beds. We will consider one dimensional conduction through a randomly packed bed sandwiched between two parallel differentially-heated plates. This configuration is frequently used to measure the so-called stagnant thermal conductivity of fully-saturated packed beds. The conductivity is formally obtained by dividing the measured net heat flux by the imposed temperature gradient between the plates. A literature survey of

heat transfer experiments in packed beds [12–18] reveals that there are significant difficulties in predicting accurately the stagnant thermal conductivity of the solid–fluid medium. Two factors contribute to this difficulty: (i) packing disorder; and (ii) boundary effect. In the following, we investigate the influence of both factors on the temperature profile and overall heat flux. Steady and unsteady heat conduction are examined separately. Finally, estimates of the overall thermal conductivity are obtained and compared with available experimental data.

MATHEMATICAL FORMULATION

The mathematical formulation of the heat conduction problem in fully-saturated packed beds is based on a homogenized description of the solid–fluid medium. Making the assumption of local thermal equilibrium, a single energy equation is derived by averaging the energy equations for two phases over a Representative Elementary Volume (REV). The size of the REV defines the characteristic spatial scale for volumetric averaging. We may note in passing that volume averages are equivalent to the more formal ensemble averages [8] only when the size of the REV is much larger than the pertinent spatial correlation scale.

We will consider a packed bed consisting of identical spherical beads stacked together 'at random'. This 'at random' is relative. Since it belongs to a stable heap, each bead has an average of 12 closest neighbors [3]; we have short-range order. Away from solid boundaries, the volumetric average of the void fraction or porosity (percentage of interstitial space) over a long slender columnar REV does not depend on its location (homogeneity) and the orientation of its axis (isotropy). In this bulk region, we can claim macroscopic disorder. In regions where the packed bed is in contact with smooth walls, the macroscopic disorder is removed and the distribution of beads is affected by the presence of the solid boundaries. Here, we focus on packed beds contained in the space between two parallel walls, as depicted in Fig. 1(a). Cheng [16] has studied the boundary effect due to the presence of the walls from a deterministic viewpoint. We can safely assume that the statistical distribution of the packing density (or porosity) remains invariant along single planes parallel to the two walls. This is equivalent to defining planar REVs parallel to the walls, as shown in Fig. 1(a). We can then account for the boundary effect by allowing the statistical distribution of medium properties (porosity and conductivity) to vary in the direction normal to the wall.

Steady state problem

Consider the problem of one-dimensional steady heat conduction in a randomly packed bed between two parallel solid walls, as depicted in Fig. 1(a). The temperatures of the walls are T_c (at $x = 0$) and T_h (at $x = 2H$). The width of the bed is $2H$. We denote by

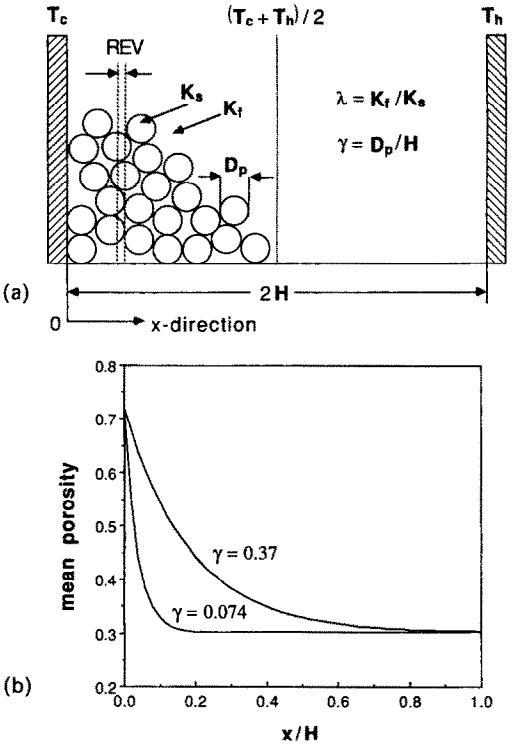

FIG. 1. (a) Schematic of the packed bed and a Representative Elementary Volume (REV). (b) Mean porosity distribution for two D_p/H values.

K_s and K_f the conductivities of the solid and fluid phase, respectively. All beads have uniform diameter D_p. Two important parameters are involved in this study. One is λ, the ratio of K_f and K_s, the other is γ, the ratio of D_p and H. We assume that the porosity distribution of this problem is symmetric with respect to the center line at $x = H$. Therefore, only half of the problem ($0 \leqslant x \leqslant H$) needs to be considered.

By aligning the bed so that the gravity vector is pointing towards the negative x-direction, we can ascertain that the fluid remains practically stagnant in the interstitial space and therefore conduction is the only mode of heat transfer. We can describe the temperature field by the following 'effective' equation for the homogenized medium (solid matrix–fluid)

$$\frac{\partial}{\partial x}\left(K_x \frac{\partial T}{\partial x}\right) = 0 \tag{1}$$

with the boundary conditions

$$T = T_c \quad \text{at } x = 0 \tag{2}$$

$$T = (T_c + T_h)/2 \quad \text{at } x = H. \tag{3}$$

K_x is the local effective conductivity which in general, is a function of position x.

There are many (occasionally diverging) opinions on the issue of defining K_x and how to represent it in terms of the conductivity of the individual phases (K_s, K_f) or the structure of the packed bed. Since we intend to focus on property randomness and the non-uniform porosity effects on the temperature distribution,

we simply adopt the empirical formula of Zehner and Schlunder [13] for a packed-sphere bed:

$$K_x = K_f\left\{[1-\sqrt{(1-\phi)}] + \frac{2\sqrt{(1-\phi)}}{1-\lambda B}\left[\frac{(1-\lambda)B}{(1-\lambda B)^2}\ln\left(\frac{1}{\lambda B}\right) - \frac{B+1}{2} - \frac{B-1}{1-\lambda B}\right]\right\} \quad (4)$$

where ϕ is the local porosity and the following expression is recommended for spherical beads:

$$B = 1.25\left[\frac{1-\phi}{\phi}\right]^{10/9}. \quad (5)$$

The above formula has been shown to give reasonable results when the wall effect is taken into account, cf. Cheng [16].

The spatial non-uniformity of porosity ϕ is a key feature of our model. In most of the porous media-related experiments, porosity is measured by using various sampling techniques. Since the beads are randomly packed, each location in the container will not be occupied by identical configurations of beads during every packing. We assume that the porosity profile is a random function of position. In the theory of random processes, one packing constitutes a single realization. All the realizations compose a random space. The outcome of each packing, i.e. the porosity, is then a random variable defined on the random space. In the context of volumetric averaging, this is equivalent to considering the porosity distribution along a planar REV depicted in Fig. 1(a). The statistical parameters of the distribution are functions of x. For a given x-location, the statistical parameters can be obtained by sampling in the corresponding REV, i.e. by considering the distribution along the plane at a distance x from the wall.

It is well known that the porosity is a strong function of x near the solid wall and that it remains almost uniform (constant) a few bead diameters away from the container wall (core region). Using the results of Haughey and Beveridge [3], Georgiadis and Catton [19] showed that in the core region, the random variations of porosity can be approximated by the Beta distribution. The following porosity profile satisfies all the above requirements:

$$\phi = \bar{\phi}(x) + \tilde{\phi} - \langle\tilde{\phi}\rangle \quad (6)$$

where

$$\bar{\phi}(x) = \phi_0\left[1 + a\exp\left(-\frac{bx}{\gamma H}\right)\right] \quad (0 \leqslant x \leqslant H) \quad (7)$$

is the deterministic component of the porosity, $a = 1.4$, $b = 2.0$, and $\phi_0 = 0.3$. The random variable $\tilde{\phi}$ accounts for the random variation of the porosity, and $\langle\tilde{\phi}\rangle$ is the mean value of $\tilde{\phi}$. Equation (6) implies that the mean porosity $\langle\phi\rangle$ is equivalent to the deterministic porosity $\bar{\phi}(x)$. The probability density function of the porosity variation is the Beta distribution with zero mean:

$$f(\tilde{\phi}) = \frac{\Gamma(\alpha+\beta)}{\Gamma(\alpha)\Gamma(\beta)}\tilde{\phi}^{\alpha-1}(1-\tilde{\phi})^{\beta-1} \quad (8)$$

where $\alpha = 32.30$ and $\beta = 56.49$. The standard deviation of the total porosity is 0.05077. cf. Georgiadis and Catton [19]. In the absence of pertinent experimental data, we have made the tacit assumption that the statistics of the local porosity fluctuation are described by the same Beta distribution (equation (8)) everywhere.

The mean porosity profiles we use in this work are plotted in Fig. 1(b) for two different bead diameter to bed thickness ratios. It is clear that when $\gamma = 0.37$, the wall effect on the porosity is much more severe than that of $\gamma = 0.074$. The standard deviation of the porosity is assumed to be the same for all positions and has the value of 0.05077 as we have mentioned previously.

An analytical solution of the system defined by equations (1)–(3) can be easily found:

$$\theta(X,\tilde{\phi}) = \frac{T-T_c}{T_h-T_c} = \frac{\int_0^X \frac{d\tau}{K_x(\tau,\tilde{\phi})}}{2\int_0^1 \frac{d\tau}{K_x(\tau,\tilde{\phi})}}. \quad (9)$$

The heat flux at the wall and the overall conductivity are given below:

$$q(\tilde{\phi}) = -K_x\frac{\partial T}{\partial x} = \frac{T_c-T_h}{2H\int_0^1 \frac{d\tau}{K_x(\tau,\tilde{\phi})}} \quad (10)$$

and

$$K_e(\tilde{\phi}) = \frac{2qH}{T_c-T_h} = \frac{1}{\int_0^1 \frac{d\tau}{K_x(\tau,\tilde{\phi})}}. \quad (11)$$

We can now obtain the expressions of the mathematical expectation and standard deviation of the above quantities:

$$E[\theta(X,\tilde{\phi})] = \int_0^1 \theta(X,\tilde{\phi})f(\tilde{\phi})\,d\tilde{\phi} \quad (12)$$

$$E[q(\tilde{\phi})] = \int_0^1 q(\tilde{\phi})f(\tilde{\phi})\,d\tilde{\phi} \quad (13)$$

$$E[K_e(\tilde{\phi})] = \int_0^1 K_e(\tilde{\phi})f(\tilde{\phi})\,d\tilde{\phi} \quad (14)$$

$$\mathrm{SD}[\theta(X,\tilde{\phi})] = \left\{\int_0^1 \{\theta(X,\tilde{\phi}) - E[\theta(X,\tilde{\phi})]\}^2 f(\tilde{\phi})\,d\tilde{\phi}\right\}^{1/2} \quad (15)$$

$$\mathrm{SD}[q(\tilde{\phi})] = \left\{ \int_0^1 \{q(\tilde{\phi}) - E[q(\tilde{\phi})]\}^2 f(\tilde{\phi})\, \mathrm{d}\tilde{\phi} \right\}^{1/2} \quad (16)$$

$$\mathrm{SD}[K_e(\tilde{\phi})] = \left\{ \int_0^1 \{K_e(\tilde{\phi}) - E[K_e(\tilde{\phi})]\}^2 f(\tilde{\phi})\, \mathrm{d}\tilde{\phi} \right\}^{1/2}. \quad (17)$$

Unsteady problem

In the unsteady heat conduction problem, all the parameters of the porosity distribution remain the same but we are faced with a more complex governing equation

$$\frac{\partial}{\partial x}\left(K_x \frac{\partial T}{\partial x}\right) = (\rho c)_m \frac{\partial T}{\partial t} \quad (18)$$

with boundary conditions

$$T = T_c \quad \text{at } x = 0 \quad (19)$$

$$T = (T_c + T_h)/2 \quad \text{at } x = H \quad (20)$$

and initial condition

$$T = (T_c + T_h)/2 \quad \text{at } t = 0. \quad (21)$$

K_x is given by equation (4), and $(\rho c)_m$ is assumed to be a constant parameter of the porous system. In a typical experiment, the initial temperature and the temperature at the walls are usually controlled. This is consistent with our assumption that the initial and boundary conditions are deterministic, as expressed by equations (19)–(21).

The non-dimensional form of the governing equations becomes

$$\frac{\partial}{\partial X}\left(K_x^* \frac{\partial \theta}{\partial X}\right) = \frac{\partial \theta}{\partial t^*} \quad (22a)$$

with

$$\theta = 0 \quad \text{at } X = 0, \quad \theta = 1/2 \quad \text{at } X = 1, \quad \text{and } \theta = 1/2 \quad \text{at } t^* = 0. \quad (22b)$$

The system of equations (22a), (23b) constitutes a well-defined initial value problem. This problem is formulated in terms of a stochastic differential equation with intrinsic randomness (since K_x^* is a random function). Hence, the solution is also expected to be a random function. We are interested in finding its mathematical expectation and standard deviation. The coupling of the random function K_x^* (which is a function of the random variable $\tilde{\phi}$) and the stochastic response θ makes the problem difficult to handle unless an explicit solution can be found, as in the case of the one-dimensional steady heat equation which we solved previously. However, an explicit solution like (9) cannot be found in closed form for the unsteady problem.

Statistical perturbation methods have been used extensively in the solution of intrinsically random systems [5–8]. Such approaches hinge on the assumption that the randomness of a parameter is small relative to its mean (or deterministic) value. This assumption decouples the random parameter from the stochastic response of the system and helps overcome the mathematical difficulty of the original problem. In general, random deviations of parameters are comparable to their mean values. Since there is no *a priori* criterion for the applicability of perturbation methods based on formal expansion techniques, a new approach has to be sought.

First, we need to discuss the details of classical numerical approaches for solving deterministic differential equations. Equation (22a) is a linear parabolic equation with variable coefficients. Employing second-order finite-difference approximation of the spatial derivatives, the simplest method for temporal integration of (22a) is the explicit (forward Euler) scheme, which is of first-order accuracy in time

$$\frac{\theta_i^n - \theta_i^{n-1}}{\Delta t} = A \frac{\theta_{i+1}^{n-1} - \theta_{i-1}^{n-1}}{2\Delta x} + D \frac{\theta_{i+1}^{n-1} - 2\theta_i^{n-1} + \theta_{i-1}^{n-1}}{(\Delta x)^2} \quad (23)$$

where Δx and Δt are the mesh size and the time step, respectively, so that $X = i\Delta x$ and $t^* = n\Delta t$. The coefficients A and D are functions of the random variable $\tilde{\phi}$ and are defined as follows:

$$A(\tilde{\phi}) = \left.\frac{\partial K_x^*}{\partial X}\right|_{X = i\Delta x} \quad (24)$$

$$D(\tilde{\phi}) = K_x^*|_{X = i\Delta x}. \quad (25)$$

The Lax equivalence theorem states that, for a well-posed initial-value problem, stability is a necessary and sufficient condition for convergence. The stability conditions for the scheme given by equation (23) are given by Peyret and Taylor [20]

$$\frac{A^2 \Delta t}{2D} \leqslant 1 \quad \text{and} \quad \frac{2D\Delta t}{(\Delta x)^2} \leqslant 1. \quad (26)$$

By rearranging equation (23) we have

$$\theta_i^n = \Delta t\left[-\frac{A}{2\Delta x} + \frac{D}{(\Delta x)^2}\right]\theta_{i-1}^{n-1} + \left[-\frac{2\Delta t D}{(\Delta x)^2} + 1\right]\theta_i^{n-1} + \Delta t\left[\frac{A}{2\Delta x} + \frac{D}{(\Delta x)^2}\right]\theta_{i+1}^{n-1}$$

$$(i = 2, 3, \ldots, N_x - 1; \quad n = 2, 3, \ldots, N_t) \quad (27)$$

where (N_x, N_t) is the total number of grid points in the (X, t^*) space. The grid-function θ_i^n in equation (27) represents $\theta(i\Delta x, n\Delta t)$ in equation (22). The initial and boundary conditions corresponding to (22b) are

$$\theta_i^1 = 1/2 \quad (i = 1, 2, \ldots, N_x) \quad (28)$$

$$\theta_i^n = 0, \ \theta_{N_x}^n = 1/2 \quad (n = 1, 2, \ldots, N_t). \quad (29)$$

If this was a deterministic problem, i.e. if K_x^* was not a random function, the numerical scheme expressed by equations (27)–(29) would be easily coded using a conventional language (FORTRAN or C) and executed on a digital computer. Now that we have the extra random variable $\tilde{\phi}$, we need to invent a procedure so that the solution is obtained explicitly, keeping at the same time the functional dependence on the random variable. Since the solution is given only numerically, we are motivated to consider (for the first time) the marriage of numerical and symbolic manipulation methods. The idea is to use symbolic computation to obtain an explict form of the solution with $\tilde{\phi}$ as a parameter. The details of our approach are given in the next section.

NUMERICAL–SYMBOLIC COMPUTATION

Symbolic computation is being increasingly used in various areas of fluid mechanics and heat transfer, cf. Bau *et al.* [21]. Unlike the classical numerical computation approach which manipulates numbers, symbolic computation provides the user with tools to manipulate mathematical expressions symbolically. Some examples include manipulating algebraic and trigonometric expressions, integrating and differentiating analytical functions and solving differential equations analytically under some special cases. There are currently several symbolic manipulators available commerically, e.g. REDUCE, MACSYMA, MATHEMATICA and MAPLE. They all have built-in capabilities of performing routine mathematical operations as well as executing algorithms supplied by the user. Since symbolic manipulators perform exact mathematical operations, they have been mostly used for solving analytical equations and deriving perturbation expansions, tasks that would otherwise require tremendous amounts of 'paper and pencil' work.

In this study, we explore a new way of applying symbolic computation to certain stochastic problems which broadens its applicability to engineering problems. We use symbolic computation to solve the one-dimensional unsteady heat conduction equation with variable and random conductivity. It will become obvious that this approach does not have to be restricted to the solution of the heat conduction equation only. In principle, it can be applied to any differential equation with random parameters (coefficients) that is amendable to numerical integration.

In the stochastic modeling of engineering problems, we are usually interested in the mathematical expectation and the variance of the solution. In the previous section, we found analytical solutions for the one-dimensional steady heat conduction problem (equations (9)–(11)). We note that the simplest way of finding the mathematical expectation or the standard deviation of these quantities is by forming certain integrals with respect to the random variable $\tilde{\phi}$, as in equations (12)–(17). Lacking similar explicit solutions for the unsteady case, we can instead manipulate equations (27)–(29), which are explicit finite-difference approximations of the solution, by using symbolic algebra. Recall that $\theta(X, t^*)$ is approximated by θ_i^n which is computed by marching forward in time. On the right hand side of equation (27), Δx, Δt are fixed and θ_{i-1}^{n-1}, θ_i^{n-1}, θ_{i+1}^{n-1} are known functions of $\tilde{\phi}$ from the previous time step. The coefficients A, D (defined by equations (24) and (25)) are also functions of the random variable $\tilde{\phi}$. Therefore, formal application of equation (27) yields θ_i^n as a function of $\tilde{\phi}$ at every time step. The random variable $\tilde{\phi}$, which is involved in the definition of the coefficients A and D (and consequently in θ_i^n via equation (27)), enters the problem through a functional relationship. The role of symbolic computation is to obtain this functional relationship *in explicit form* throughout the numerical integration via (27).

We used the symbolic manipulation software package MAPLE (Version 4.2.) [22] on a Sun 3 workstation. In the following, we briefly outline the coupled numerical–symbolic scheme for the solution of (22a), (22b).

1. Read input parameters γ, λ, K_f, a, b, ϕ_0, Δx, Δt.
2. Read functional expressions $\phi(x, \tilde{\phi})$, $K_x(\phi)$.
3. Evaluate coefficients involved in the governing equation (22a), in this case K_x^*.
4. Develop finite-difference approximations for

$$\frac{\partial \theta}{\partial t^*}, \quad \frac{\partial^2 \theta}{\partial X^2} \quad \text{and} \quad \frac{\partial \theta}{\partial X}.$$

5. Read initial and boundary conditions. Derive explicit form for each time step, as in equations (27)–(29).
6. March forward in time using symbolic manipulations software. Store results for every time step in Array-D.
7. Read in the probability density function of the random variable, equation (8).
8. Compute the mathematical expectation and standard deviation for each element of Array-D and store in Array-E and Array-SD, respectively.

Each element of Array-D, which is computed in step 6, is a function of the random variable $\tilde{\phi}$. Generally, numerical integrations have to be performed in step 8 since the solution is not available in closed-form. MAPLE has the additional feature of numerical integration. In reality, since the expression of each integral can contain thousands of terms, the RAM space of the Sun 3 computer we used is not enough to complete the whole computation. It is almost impossible to accomplish a job with arrays having more than 10×10 elements. Here, we used additionally a Cray Y-MP computer to do the numerical integrations with a FORTRAN code. Since the typical number of elements in the Array-D is of order 10^4, we had to partition the arrays. Every ten time steps, we had to store the results from step 6 to Array-D, transfer to

the Cray for the integrations of step 8, transfer the results back to the Sun workstation, and use them as initial conditions for the next 10 steps. The results eventually converge to the steady state solution as we show in the following section.

RESULTS AND DISCUSSION

The results for the steady case have been summarized in Figs. 2–5 and Tables 1 and 2. In all the figures, only half of the packed beds domain is shown due to the symmetry with respect to the center line. We examined five different combinations: oil/glass, water/steel, glycol/steel, glycol/acrylic and water/acrylic. The thermal conductivities of the solid and fluid phases are listed in Table 1. For each medium, two geometries have been studied, $\gamma = 0.37$, where the bed width is about 6 times the bead diameter; and $\gamma = 0.074$, where the bed width is about 28 times the bead diameter. It is known that wall effect on the porosity distribution is felt inside a layer which is about four bead diameters thick; the reader is referred to Fig. 1(b). Our results show that the heat conduction characteristics in the packed beds depend on both λ and γ.

The local effective conductivity computed from equations (4) and (5) has a mean value that is plotted in Figs. 2(a) and 3(a). Its standard deviation is plotted

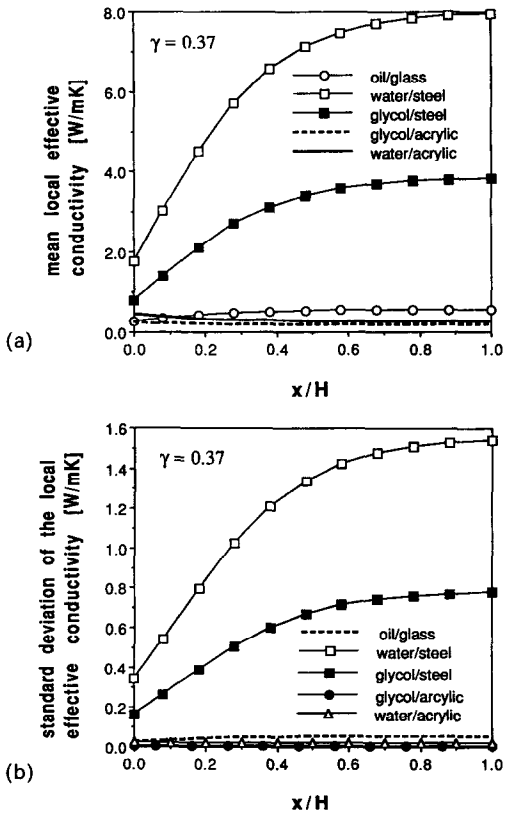

FIG. 2. Local effective conductivity for $\gamma = 0.37$. (a) Mean value; (b) standard deviation.

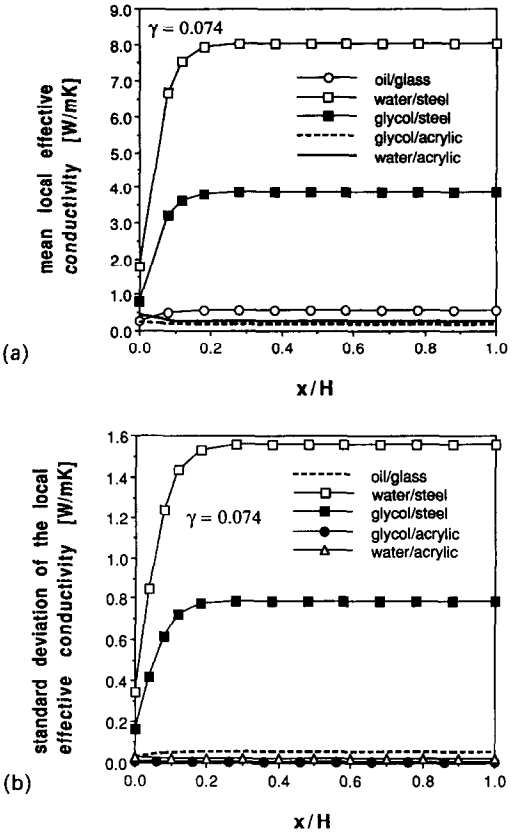

FIG. 3. Local effective conductivity for $\gamma = 0.074$. (a) Mean value; (b) standard deviation.

in Figs. 2(b) and 3(b). For the same medium, the wall effect on the mean of the local conductivity increases as the value of γ increases. For the same geometry, the wall effect is more important for combinations with λ much less than $O(1)$, such as water/steel and glycol/steel. The standard deviation of the local effective conductivity shows the same trends. It is worth noting that the deviation can reach as much as 20% of the mean value.

Figures 4(a), 5(a) give the mean value of the temperature profile. For media with $\lambda \ll 1$ and $\gamma = 0.37$ (Fig. 4(a)), wall effects are strongly manifested by large temperature gradients near the solid wall. The closer λ is to unity, the weaker the wall effect is. This result agrees with the analysis of Cheng [16]. However, if λ exceeds 1, the wall is felt again, but this time, the temperature profile has the opposite curvature from the $\lambda \ll 1$ case, and there is a smaller temperature drop near the wall. This phenomenon is not observed in Cheng's [16] deterministic model. For $\gamma = 0.074$ (Fig. 5(a)), the wall effect is same, only weaker. The standard deviation of the temperature is plotted in Figs. 4(b), 5(b). Observe that the standard deviation is zero both on the wall ($x = 0$) and the center line ($x = H$). This is a result of deterministic boundary conditions and the imposed symmetry of the problem. The standard deviation reaches its maximum value nearer to the wall for the smaller γ case. However, one should

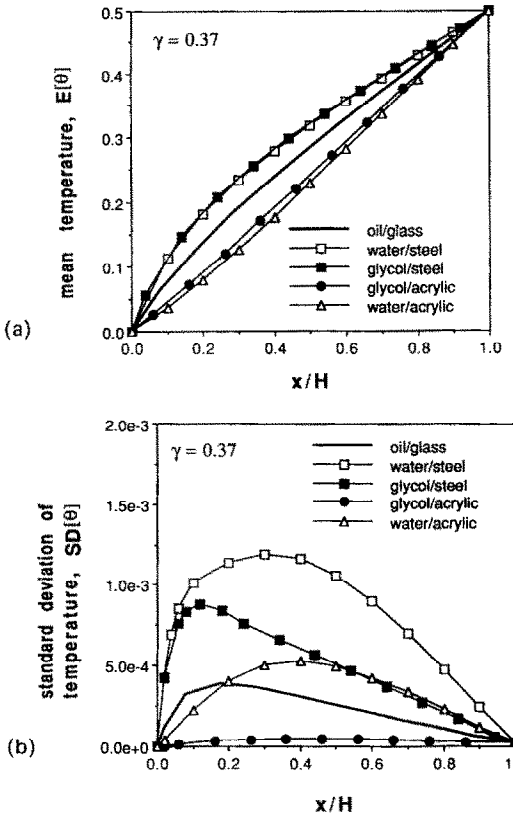

Fig. 4. Dimensionless temperature distribution for $\gamma = 0.37$. (a) Mean value; (b) standard deviation.

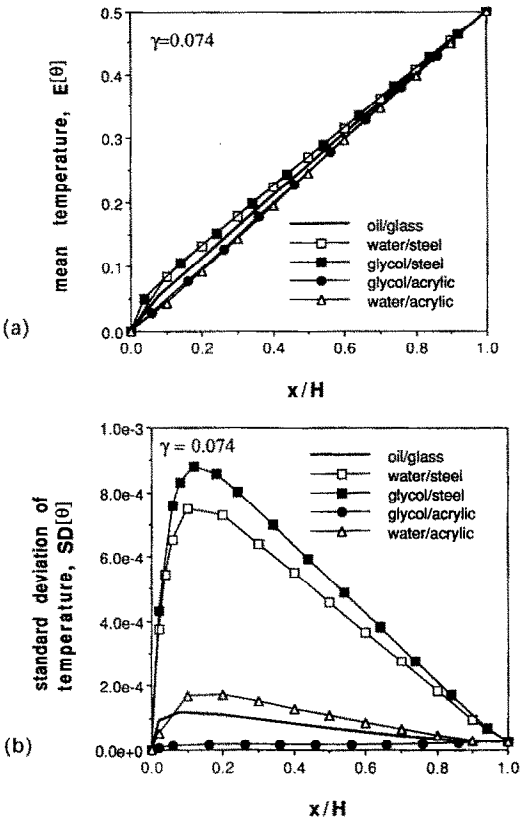

Fig. 5. Dimensionless temperature distribution for $\gamma = 0.074$. (a) Mean value; (b) standard deviation.

note that the temperature deviation is only about 10^{-3} relative to its mean value.

The mean values and standard deviations of the net heat flux and the *overall* effective conductivity, are compiled in Table 1 for the same five combinations of media and two γ values. In Table 2, we repeat the computed conductivity results for each reference (the two values separated by a slash correspond to $\gamma = 0.37$ and $\gamma = 0.074$). We also list the range of experimental estimates of conductivity found in the literature [12,

Table 1. Computed results of average total heat flux, average overall conductivity and their standard deviations

					$\gamma = D_p/H = 0.37$				$\gamma = D_p/H = 0.074$			
Liquid	Solid	K_f	K_s	λ	$\langle q \rangle$	SD[q]	$\langle K_e \rangle$	SD[K_e]	$\langle q \rangle$	SD[q]	$\langle K_e \rangle$	SD[K_e]
Oil	Glass	0.15	1.1	0.136	0.241	0.023	0.481	0.046	0.274	0.026	0.548	0.052
Water	Steel	0.615	63.18	0.01	2.8	0.519	5.599	1.039	3.689	0.709	7.378	1.417
Glycol	Steel	0.262	37.39	0.007	1.320	0.256	2.641	0.512	1.766	0.356	3.532	0.712
Glycol	Acrylic	0.261	0.16	1.63	0.097	0.002	0.194	0.005	0.094	0.002	0.188	0.005
Water	Acrylic	0.63	0.16	3.937	0.143	0.01	0.287	0.02	0.133	0.009	0.266	0.019

Table 2. Comparison of computed overall conductivity $\langle K_e \rangle$, maximum theoretical estimate K_e max, and experimental results K_e exp from refs. [12, 14, 15, 17]. The values separated by slash correspond to $\gamma = 0.37/\gamma = 0.074$

Liquid	Solid	λ	$\langle K_e \rangle$	SD[K_e]	K_e max	K_e exp
Oil	Glass	0.136	0.481/0.548	0.046/0.052	0.742/0.8	0.47–0.60
Water	Steel	0.01	5.599/7.378	1.039/1.417	39.57/43.44	3.30–4.88
Glycol	Steel	0.007	2.641/3.532	0.512/0.712	23.38/25.68	1.87–2.58
Glycol	Acrylic	1.63	0.194/0.188	0.005/0.005	0.198/0.192	0.21 0.22
Water	Acrylic	3.937	0.287/0.266	0.02/0.019	0.337/0.308	0.36–0.48

14, 15, 17], as well as an 'upper bound' for the conductivity of an equivalent homogeneous packed bed given by the following expression

$$K_e \max = \Phi K_f + (1-\Phi)K_s \qquad (30)$$

Φ is an average porosity obtained by averaging equation (7) over the channel width. The two values separated by a slash and listed under the column K_e max in Table 2 correspond to $\Phi = 0.377$ ($\gamma = 0.37$) and $\Phi = 0.316$ ($\gamma = 0.074$).

Our computations imply that the standard deviation in effective conductivity can be as high as 20% of the mean value for combinations with $\lambda \ll 1$. This exceeds the typical 5–10% experimental error in reported conductivity measurements [14, 15] and is consistent with the wide scatter of experimental values for water/steel packed beds. Another observation concerns the $\lambda > 1$ case. Nield [18] has called attention to the fact that the measured values by Prasad *et al.* [17] exceed the 'upper bound' K_e max. Our results in Table 2 for glycol/acrylic and water/acrylic explain at least part of this anomaly. They indicate that the difference between the expected value $\langle K_e \rangle$ and K_e max is about one standard deviation.

A plot of the unsteady temperature profiles is given in Figs. 6(a)–(c). The mesh size Δx chosen is 0.1 and the time step Δt is 0.0009, in order to satisfy the stability conditions (given by equation (6)). Only the simulation for the combination water/steel with $\gamma = 0.37$ is performed. We have only shown the first 190 time steps for both the mean temperature field (Fig. 6(a)) and its standard deviation (Figs. 6(b), (c)). The mean temperature field reveals the monotonic approach of the transient profile from the initially uniform distribution to the steady state solution. Figure 6(b) shows the large spike in the standard deviation distribution at the onset. Figure 6(c) gives a detailed plot of the standard deviation profiles for large times. The deviation seems to approach the steady state profile in a non-monotonic fashion. For each time step, the computation typically takes an hour of CPU time on the Sun 3 workstation. Therefore, extensive calculations using the current configuration are difficult at the moment.

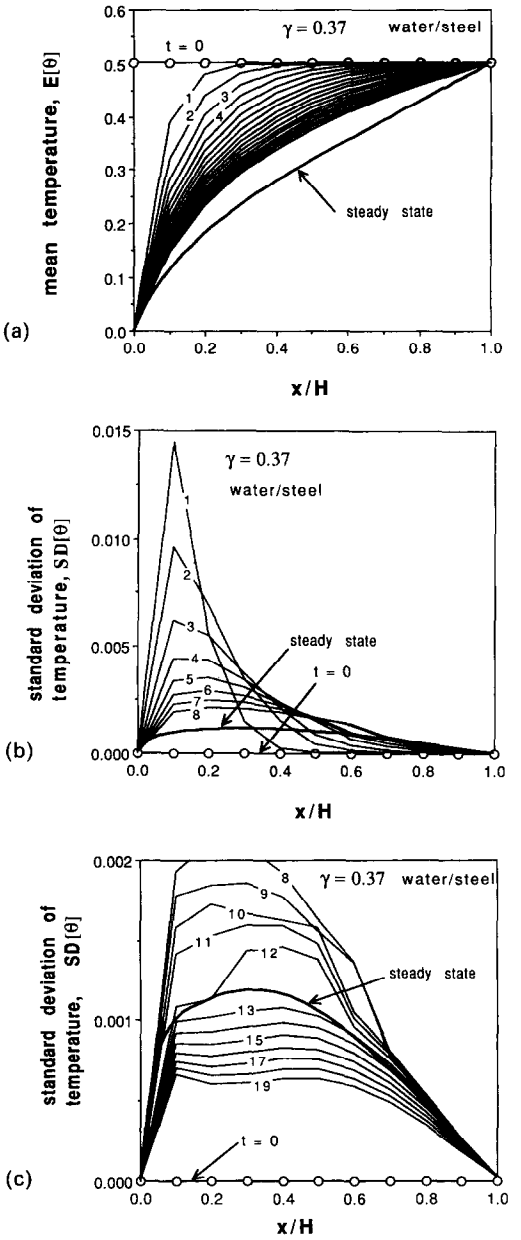

FIG. 6. Transient temperature distribution for $\gamma = 0.37$. (a) Mean value; (b) standard deviation; (c) standard deviation close-up. Each profile in (b) and (c) is marked by a number which denotes the time instant in $10\Delta t$ units, i.e. curve 19 corresponds to $t = 190\Delta t$.

CONCLUDING REMARKS

For the first time (according to the present authors' knowledge), a combination of a numerical scheme and symbolic manipulation software has been used to solve a parabolic transport equation with random conductivity. The equation is discretized on a finite spatial grid and an explicit integration in time is carried out symbolically for each time step. Although our example involves the heat equation in a single spatial dimension, this approach can be, in principle, extended to solve a broader class of stochastic partial differential equations with random coefficients. More than one spatial dimensions can be handled provided explicit temporal schemes are constructed. This seems feasible if the symbolic manipulation is carried out on a supercomputer.

The feasibility of a direct computation of the statistical mean and standard deviation for both steady and unsteady conduction is demonstrated. Such simulations provide valuable insight into the complex dynamics of stochastic processes. In addition, the standard deviation can reveal the reliability of the mean value when used in engineering estimates. In the particular case of effective thermal conductivity of packed beds, we proved that the computed standard deviation provides an *a priori* estimate of error.

In closing, we have proposed a *general* direct method for the solution of stochastic problems governed by partial differential equations with intrinsic randomness. The physical problem we chose does not necessarily demonstrate the superiority of this approach compared to perturbation schemes [6–8]. Perturbation schemes based on formal asymptotic expansions still offer an economic alternative provided their convergence is demonstrated.

Acknowledgements—Xiaowei He would like to acknowledge the financial support of the NSF/Duke Engineering Research Center for Emerging Cardiovascular Technologies under a Graduate Fellowship. The work of John Georgiadis is partially supported by the U.S. Dept. of Energy (grant DE-FG05-90ER14141) and the National Science Foundation (grants CTS-8909119 and CTS-9006189). Both authors are also indebted to the North Carolina Supercomputing Center for a generous allocation of computer resources.

REFERENCES

1. E. Vanmarcke, *Random Fields*. MIT Press, Cambridge MA (1983).
2. J. G. Georgiadis, Future research needs in heat and mass transport in porous media. In *Convective Heat and Mass Transfer in Porous Media* (Edited by S. Kakaç, B. Kilkis, F. A. Kulacki and F. Arinç), NATO ASI-series, Vol. E 196, pp. 1073–1088. Kluwer Academic Publishers, The Netherlands (1991).
3. D. P. Haughey and G. S. G. Beveridge, Local voidage variation in a randomly packed bed of equal-sized spheres, *Chem. Engng Sci.* **21,** 905–916 (1966).
4. G. Sposito, W. A. Jury and V. K. Gupta, Fundamental problems in the stochastic convection-dispersion model of solute transport in aquifers and field soils, *Water Resour. Res.* **22**(1), 77–78 (1986).
5. H. Benaroya and M. Rehak, Finite element methods in probabilistic structural analysis: A selective review, *Appl. Mech. Rev.* **41**(5), 201–213 (1988).
6. D. Y. Tzou, Stochastic analysis of temperature distribution in a solid with random heat conductivity, *J. Heat Transfer* **110,** 23–29 (1988).
7. D. Y. Tzou, Stochastic modelling for the contact problems in heat conduction, *Int. J. Heat Mass Transfer* **32,** 913–921 (1989).
8. J. G. Georgiadis, On the approximate solution of nondeterministic heat and mass transport problems, *Int. J. Heat Mass Transfer* **34,** 2190–2198 (1991).
9. S. Torquato, Electrical conductivity of two-phase disordered composite media, *J. Appl. Phys.* **58,** 3790–3797 (1985).
10. J. Padovan and Y. H. Guo, Solution of nondeterministic finite element and finite difference heat conduction simulations, *Numerical Heat Transfer A* **15,** 383–398 (1989).
11. J. Padovan, Y. H. Guo and G. Ryland, Static response of sparsely probabilistic systems, preprint, Dept Mechanical Engineering, University of Akron (1990).
12. M. Combarnous, Convection naturelle et convection mixte en milieu poreux, Doctral Dissertation, University of Paris (1970).
13. P. Zehner and E. U. Schlunder, Thermal conductivity of granular materials at moderate temperature (in German), *Chemie Ing. Techn.* **42,** 933–941 (1970).
14. G. W. Somerton, Natural convection and boiling in porous media, Ph.D. Thesis, University of California at Los Angeles (1982).
15. T. Jonsson and I. Catton, Effect of Prandtl number dependence of Benard convection in porous media, *J. Heat Transfer* **109,** 371 (1987).
16. P. Cheng, Heat conduction on a packed beds with wall effect, *Int. Commun. Heat Mass Transfer* **13,** 11–21 (1986).
17. V. Prasad, N. Kladias, A. Bandyopadhaya and Q. Tian, Evaluation of correlations for stagnant thermal conductivity of liquid-saturated porous beds of spheres, *Int. J. Heat Mass Transfer* **32**(9), 1793–1796 (1989).
18. D. A. Nield, Estimation of the stagnant thermal conductivity of saturated porous media, *Int. J. Heat Mass Transfer* **34**(6), 1575–1576 (1991).
19. J. G. Georgiadis and I. Catton, Stochastic modelling of unidirectional fluid transport in uniform and random packed beds, *Physics Fluids* **30**(4), 1017–1022 (1987).
20. R. Peyret and T. D. Taylor, *Computational Methods for Fluid Flow* (2nd Print), p. 40. Springer, New York (1985).
21. H. H. Bau, T. Herbert and M. M. Yovanovich (Eds), *Symbolic Computation in Fluid Mechanics and Heat Transfer*, HTD-Vol. 105, AMD-Vol. 97. ASME, New York (1988).
22. B. W. Char, *MAPLE Reference Manual* (5th Edition). University of Waterloo, Canada (1988).

SOLUTION NUMERIQUE DIRECTE DES PROBLEMES DE DIFFUSION AVEC UN ERREMENT INTRISEQUE

Résumé—Un schéma de manipulation hydride numérique-symbolique est développé pour l'analyse des problèmes de diffusion avec errement intrisèque. Le schéma est appliqué à l'étude de la conduction thermique monodimensionnelle dans des lits fixes pleinement saturés de façon à étudier les effets du désordre de l'empilement sur la conductivité effective du milieu. La conduction est modélisée par une équation parabolique aux dérivées partielles avec une conductivité locale aléatoire. Le hasard provient de la fluctuation spatiale de la porosité près des parois solides et dans la région du coeur. En supposant une certaine distribution statistique de porosité, les problèmes de conduction permanente et variable sont résolus. La solution permanente est utilisée pour obtenir à la fois la valeur moyenne et l'écart-type de la conductivité effective pour un domaine du rapport des conductivités du fluide et du solide. La moyenne et l'écart-type sont utilisés pour interpréter la dispersion des résultats expérimentaux trouvés dans la littérature. L'équation de la conduction thermique variable est discrétisée sur une grille spatiale finie et une intégration explicite dans le temps et conduite symboliquement pour chaque pas de temps.

DIREKTE NUMERISCHE LÖSUNG VON DIFFUSIONSPROBLEMEN MIT ZUFALLSCHARAKTER

Zusammenfassung—Es wird eine hybride numerisch-symbolische Vorgehensweise bei der Analyse von Diffusionsproblemen mit Zufallscharakter entwickelt. Das Verfahren wird auf die Untersuchung der eindimensionalen Wärmeleitung in vollständig gesättigten Festbetten angewandt, um den Einfluß der Packungs-Unordnung auf die effektive Wärmeleitfähigkeit zu bestimmen. Der Leitvorgang wird mittels einer parabolischen partiellen Differentialgleichung mit zufälliger örtlicher Leitfähigkeit modelliert. Der Zufallscharakter rührt von der örtlichen Schwankung der Porosität nahe der festen Begrenzungswand und im Kerngebiet her. Unter der Voraussetzung einer bestimmten statistischen Verteilung der Porosität werden stationäre und instationäre Wärmeleitungsprobleme gelöst. Mit Hilfe der stationären Lösung ergibt sich sowohl der Mittelwert als auch die Standardabweichung der effektiven Wärmeleitfähigkeit in einem weiten Bereich des Wärmeleitfähigkeitsverhältnisses von Fluid und Feststoff. Mittelwert und Standardabweichung werden für die Interpretation der Streuung von Versuchsergebnissen aus der Literatur verwendet. Die Gleichung für die instationäre Wärmeleitung wird in ein endliches räumliches Gitter diskretisiert. Die explizite Integration über die Zeit wird symbolisch für jeden Zeitschritt ausgeführt.

ПРЯМОЕ ЧИСЛЕННОЕ РЕШЕНИЕ ЗАДАЧ ДИФФУЗИИ С ВНУТРЕННЕЙ ХАОТИЗАЦИЕЙ

Аннотация—Для анализа задач диффузии с внутренней хаотизацией разработана гибридная схема численно-операторных преобразований. Схема используется при исследовании одномерной теплопроводности в полностью насыщенных плотных слоях с целью изучения влияния неупорядоченности упаковки на эффективный коэффициент теплопроводности среды. Теплопроводность моделируется параболическим уравнением в частных производных со случайным локальным коэффициентом теплопроводности. Хаотичность возникает вследствие пространственных флуктуаций порозности у твердых стенок и в объеме. В предположении статистического распределения порозности решаются стационарные и нестационарные задачи теплопроводности. Стационарное решение используется для нахождения среднего значения и стандартного отклонения эффективного коэффициента теплопроводности в исследуемом диапазоне отношений теплопроводностей жидкости и твердого тела. Среднее и стандартное отклонения используются для объяснения разброса имеющихся в литературе экспериментальных данных. Нестационарное уравнение теплопроводности дискретизируется с помощью пространственной сетки, и операторным методом осуществляется интегрирование на каждом временном шаге.